

The Contribution of Field OB Stars to the Ionization of the Diffuse Ionized Gas in M33^{1,2}

Charles G. Hoopes and René A. M. Walterbos³

*New Mexico State University, Department of Astronomy, MSC4500, Box 30001
Las Cruces, New Mexico 88003*

choopes@NMSU.edu, rwalterb@NMSU.edu

ABSTRACT

We present a study of the ionizing stars associated with the diffuse ionized gas (DIG) and HII regions in the nearby spiral galaxy M33. We compare our Schmidt H α image to the far-ultraviolet (FUV, 1520 Å) image from the Ultraviolet Imaging Telescope (UIT). The H α /FUV ratio is higher in HII regions than in the DIG, suggesting an older population of ionizing stars in the DIG. Assuming ionization equilibrium, we convert the H α flux to the number of Lyman continuum photons $N_{Ly\alpha}$. When compared to models of evolving stellar populations, the $N_{Ly\alpha}$ /FUV ratio in HII regions is consistent with a young burst, while the DIG ratio resembles an older burst population, or a steady state population built up by constant star formation, which is probably a more accurate description of the stellar population in the field. The UIT data is complimented with archival FUV and optical images of a small portion of the disk of M33 obtained with WFPC2 on HST. These images overlap low- and mid-luminosity HII regions as well as DIG, so we can investigate the stellar population in these environments. Using the HST FUV and optical photometry, we assign spectral types to the stars observed in DIG and HII regions. The photometry indicates that ionizing stars are present in the DIG. We compare the predicted ionizing flux with the amount required to produce the observed H α emission, and find that field OB stars in the HST images can account for $40\% \pm 12\%$ of the ionization of the DIG, while the stars in HII regions can provide $107\% \pm 26\%$ of the H α luminosity of the HII regions. Due to the limited coverage of the HST data, we cannot determine if stars outside the HST fields ionize some of the DIG located in the HST fields, nor can we determine if photons from stars inside the HST fields leak out of the area covered by the HST fields. We do not find any correlation between leakage of ionizing photons and H α luminosity for the HII regions in our HST fields. However,

³Visiting Astronomer, Kitt Peak National Observatory, National Optical Astronomy Observatories, which is operated by the Association of Universities for Research in Astronomy, Inc. (AURA) under cooperative agreement with the National Science Foundation.

the HST fields do not include very luminous HII regions, and it would be worthwhile to see if there is any trend at higher luminosities. If stellar photons alone are responsible for ionizing the DIG, the current results are consistent with no or few ionizing photons escaping from the galaxy.

Subject headings: Galaxies: Individual (M33) — Galaxies: ISM — Galaxies: Spiral — Galaxies: Star Clusters — Stars: Early-type — Stars: Formation

1. Introduction

An important component of the interstellar medium (ISM) in spiral galaxies is the diffuse ionized gas (DIG, also called WIM for warm ionized medium). DIG is a warm (~ 8000 K), diffuse ($n_e=0.1-0.2$ cm $^{-3}$) layer of ionized hydrogen which permeates the disks of spiral galaxies (see Waltherbos & Braun 1996 for a review). In the Milky Way, where it is often referred to as the Reynolds layer, DIG accounts for almost all of the ionized gas mass, contributes about 30% of the local HI column, and fills at least 20% of the volume of the galaxy (Reynolds 1991). DIG in several edge-on galaxies has been studied through H α imaging (Rand, Kulkarni, & Hester 1990; Dettmar 1990; Pildis, Bregman, & Schombert 1994; Rand 1996; Hoopes, Waltherbos, & Rand 1999), and the extent and brightness of halo DIG has been found to vary dramatically. In face-on galaxies, however, the most surprising discovery has been the *similarity* of the DIG content among galaxies spanning a large range of characteristics. The DIG components of many non-edge-on galaxies have been studied: M31 (Waltherbos & Braun 1994), M33 (Hester & Kulkarni 1990; Greenawalt 1998), M51 and M81 (Greenawalt *et al.* 1998; Wang, Heckman, & Lehnert 1997, 1999), NGC 253 and NGC 300 (Hoopes, Waltherbos, & Greenawalt 1996), NGC 247 and NGC 7793 (Ferguson *et al.* 1996), and M101 (Wang, Heckman, & Lehnert 1997, 1999; Greenawalt 1998). Despite the range of parameters seen in these galaxies, the contribution of the DIG to the total H α luminosity (the *diffuse fraction*) is consistently between 30 and 50%. This is essentially a comparison of the DIG luminosity and the HII region luminosity, so the constant ratio establishes a link between the DIG and massive star formation.

Photoionization by massive stars and shock ionization by supernovae have both been proposed as ionization sources of the DIG. All other sources have been found to lack by far the required energy (Reynolds 1984), although Webber (1998) finds that cosmic ray ionizations may be a somewhat more significant source than previously thought. The consistent diffuse fraction of 30 to 50% of the

¹Observations made with the Burrell Schmidt Telescope of the Warner and Swasey Observatory, Case Western Reserve University.

²Based on observations made with the NASA/ESA Hubble Space Telescope, obtained from the data archive at the Space Telescope Science Institute. STScI is operated by the Association of Universities for Research in Astronomy, Inc. under NASA contract NAS 5-26555.

total $H\alpha$ luminosity implies that a similar fraction of the ionizing photons produced in a galaxy is required to power the DIG, if photoionization is responsible for the DIG. The diffuse fraction for M33 is 40% (Greenawalt 1998), which leads to a minimum energy requirement (assuming all ionizing photons have $\lambda=912 \text{ \AA}$) for the DIG of $1.8 \times 10^{41} \text{ erg s}^{-1}$, or $1.7 \times 10^{-4} \text{ erg s}^{-1} \text{ cm}^{-2}$ of disk, using a radius of 6 kpc for M33. This can be compared to $1.0 \times 10^{42} \text{ erg s}^{-1}$ and $1 \times 10^{-4} \text{ erg s}^{-1} \text{ cm}^{-2}$ for the Milky Way, using a radius of 15 kpc, which just equals the amount of energy provided by supernovae (Reynolds 1984). In M33 the supernova rate is 1/360 years (Gordon, *et al.* 1998), which leads to $0.9 \times 10^{41} \text{ erg s}^{-1}$, using the canonical 10^{51} erg for each supernova. This is a factor of 2 too low to account for the DIG, even assuming an unrealistic 100% efficiency in converting the energy into ionized gas. Also, the $H\alpha$ luminosity used here has not been corrected for internal extinction, which would make the power requirement even higher. Although some DIG may be shock ionized, supernovae cannot be the source of energy responsible for the bulk of the ionization of the DIG in M33 or the Milky Way, through shock ionization or any other source which taps supernovae energy, such as turbulent mixing layers (Slavin, Shull, & Begelman 1993).

This leaves OB stars as the most likely source. Photoionization is consistent for the most part with spectroscopic observations of the DIG. Emission from [SII] 6716, 6731 \AA and [NII] 6548, 6584 \AA is enhanced relative to $H\alpha$ in the DIG when compared to HII regions, and [OIII] 4959, 5007 \AA is fainter relative to $H\beta$ (Rand 1997; Greenawalt, Walterbos, & Braun 1997; Haffner, Reynolds, & Tufte 1999; Reynolds 1985). This spectrum has been reproduced by photoionization models (Domgörgen & Mathis 1994) using a dilute radiation field in a diffuse medium. Low limits on HeI 5876 \AA / $H\alpha$ in the Milky Way (Reynolds & Tufte 1995) have yet to be explained, and in NGC 891 the HeI/ $H\alpha$ ratio, while higher than in the Milky Way, is still too low to be consistent with other line ratios (Rand 1997). In M31, however, the HeI emission is consistent with the Domgorgen & Mathis models (Greenawalt, Walterbos, & Braun 1997), at least for the brightest DIG, and the HeI/ $H\alpha$ ratio in several irregular galaxies is also consistent with photoionization (Martin & Kennicutt 1997). A more challenging problem has been posed by high [OIII]/ $H\beta$ ratios seen in the DIG of several galaxies (Wang, Heckman, & Lehnert 1997; Rand 1998), which still have not been reproduced by pure photoionization models. Nevertheless, the bulk of the evidence suggests that OB stars are the dominant ionization source for the DIG.

There is still uncertainty, however, regarding the location of the OB stars responsible for ionizing the DIG. Are the ionizing photons leaking out of density-bounded HII regions, or are there enough *field OB stars* to provide the ionizing photons? Either option is a deviation from commonly held views of the ISM. If field stars are the dominant source of ionizing photons, this requires a substantial population of massive stars outside of HII regions. Do these stars form in the field, do they manage to drift out of the cloud in which they formed, or is the gas swept away by the supernovae of even more massive stars? On the other hand, if the photons which are ionizing the DIG are leaking out of HII regions, an appreciable population of density-bounded HII regions is required. HII regions are usually treated as being radiation-bounded, which makes the determination of star formation rates from $H\alpha$ luminosities straightforward. Does such a population

of leaky HII regions exist?

Evidence for field OB stars does exist (Torres-Peimbert, Lazcano-Araujo, & Peimbert 1974; Humphreys & Sandage 1980; Garmany, Conti, & Chiosi 1982; Massey *et al.* 1995a). Massey *et al.* (1995a) defined field stars as those further from an HII region than a star could travel in the lifetime of an OB star ($< 10^7$ years), a few tens of parsecs at most. Using ground-based UVB photometry, Patel & Wilson (1995) investigated the distribution of OB stars in M33. They concluded that 50% of the ionizing stars were found outside of HII regions. Such a study is difficult using ground-based optical data, where both crowding and the color degeneracy of hot stars pose serious problems. A systematic search for field OB stars is needed, and space based photometry in the ultraviolet can provide a strong test of the optical results.

The alternative to field OB stars is a significant population of density-bounded HII regions. Individual HII regions which are density-bounded do exist, such as the Orion nebula (Rubin *et al.* 1991) and the starburst in NGC 4214 (Leitherer *et al.* 1996b). Oey & Kennicutt (1997) compared the $H\alpha$ luminosities of several HII regions in the LMC with the predicted ionizing fluxes of the stars within. They found 2 out of 14 HII regions to be substantially leaking ionizing photons, and 3 others that were slightly leaky. The observed absence of Lyman continuum radiation leaking from spirals (Leitherer *et al.* 1995) suggests that such radiation is contained within HII regions, although it is conceivable that HII regions are just leaky enough to ionize the DIG, but not so much that an appreciable number of ionizing photons escapes the entire galaxy (Wang, Heckman, & Lehnert 1997). There is evidence from the $H\alpha$ luminosity functions of HII regions in spirals that high luminosity HII regions may be density-bounded (Beckman *et al.* 2000).

Here we focus on identifying the stars responsible for ionizing the DIG. In order to isolate massive stars we turn to the far-ultraviolet (FUV), where OB stars dominate the stellar emission. The local group spiral M33 is an ideal galaxy to study the ionization of the DIG, due to its low inclination, vigorous star formation rate, and distance of only 0.84 Mpc (Freedman, Wilson, & Madore 1991). In section 2 we discuss the data used to carry out this project, which include $H\alpha$ imaging of M33, FUV imaging using the Ultraviolet Imaging Telescope (UIT), and optical and FUV stellar photometry from the Wide Field Planetary Camera 2 (WFPC2) on *Hubble Space Telescope* (HST). In section 3 we briefly review the properties of the DIG in M33. In section 4 we discuss the FUV emission on large scales from the UIT image and its relation to the $H\alpha$ emission from both DIG and HII regions. In section 5 we present the results of the stellar photometry in HII regions and DIG. In section 6 we compare the FUV information from HST and UIT. Section 7 contains a discussion of the results and conclusions.

2. The Data

2.1. The H α Mosaic

Table 1 contains a summary of the observations. The ground-based data consist of H α and off-band continuum images of M33 obtained with the 0.6 meter Burrell-Schmidt telescope at Kitt Peak National Observatory in November 1995 (Greenawalt 1998). The 2048² detector provided a field of view of 1.15 \times 1.15 degrees² at 2.028''/pixel. The images were offset using the shift-and-stare technique to minimize flat-field irregularities. The final mosaic covers an area of about 1.75 \times 1.75 degrees². We reduced the images using standard procedures in IRAF. Twilight flats from all nights of the observing run were co-added to create a “super flat” which was used to correct for gain variations. We calibrated the continuum image using the published R magnitude and the known shape and transmission of the continuum filter. The H α image was calibrated relative to the continuum, again using the shape and transmission of the line filters. The continuum image was scaled to the H α image using foreground stars and subtracted. The total H α flux we observed is 3.6×10^{-10} ergs s⁻¹ cm⁻². Spectroscopy of DIG and HII regions in M33 (Hoopes & Walterbos 2000, in preparation) shows that [NII] 6584Å emission is about 20% as strong as H α in both the DIG and HII regions. The lack of [NII] enhancement in the DIG and the lower ratios in both environments than seen in other galaxies are probably due to a lower Nitrogen abundance in M33 (Vílchez *et al.* 1988). The result is that at most only 5% of the light detected in the H α filter can arise from [NII] emission, and the amount of contamination is the same for both HII regions and DIG. The continuum-subtracted H α image is shown in figure 1.

2.2. The UIT Image

We obtained an archival UIT image of M33 taken on the *Astro-1* space shuttle mission (Stecher *et al.* 1992, 1997). We used the FUV image, a 424 second exposure taken through the B1 filter ($\lambda=1520\text{\AA}$, $\Delta\lambda=354\text{\AA}$). The image was originally produced on film and later digitized. The resolution of the image is about 3'' and the field of view is roughly 40'. The H α image was convolved to similar resolution and put on the same grid. UIT was calibrated in the laboratory before launch and also in flight by comparing UIT images with previous UV space missions. The calibration uncertainty is about 15% (Stecher *et al.* 1992). The UIT image can be found in Landsman *et al.* (1992).

2.3. WFPC2 Images and Stellar Photometry

Lastly, we used archival HST WFPC2 images of regions in M33, from project GO6038. These images were originally obtained to study hot stars and star clusters in M33 (Chandar, Bianchi, & Ford 1999). Figure 1 shows that the pointings are restricted to the inner $\sim 10'$ radius of M33, but

all of the pointings contain HII regions and DIG. The pointings near the center cover regions that are more crowded than those covered in the pointings at larger radii. Spiral arms and inter-arm regions are both sampled. The only obvious bias introduced by the locations of the images is that they do not include the brightest HII regions in M33. The filters and exposure times are F170W (2×900 s), F336W (2×900 s), F439W (600 s) and F555W (160 s). The two separate exposures in the UV and FUV filters were combined to remove cosmic rays. The images were corrected for the $\sim 4\%$ charge transfer efficiency problem of the WFPC2 by multiplying with a ramp image as described by Holtzman *et al.* (1995). The F170W and F336W images were also corrected for degradation of throughput after decontamination, again using the formula in Holtzman *et al.* (1995).

Photometry was performed on the HST images using the DAOPHOT package. For each frame, a PSF model was created using bright, isolated stars. The empirical PSF model was found using an iterative process. A constant PSF model was first computed and used to subtract the neighbors of the PSF stars. Then a linearly varying PSF model was computed on the image with the PSF neighbors subtracted, and then used to remove the PSF neighbors from the original image. Finally a quadratically varying model was computed from the PSF stars with the neighbors subtracted. If there were few PSF stars (less than about 15, which was usually the case in the F170W images) a constant psf model was used. It was also created iteratively, first making a model PSF, then subtracting any neighbors of the PSF stars and revising the PSF based on the subtracted image. We compiled a list of stars detected in all four bands. The magnitudes were put on the STMAG photometric system, described by Holtzman *et al.* (1995), using the most recently determined calibration for WFPC2. The calibration uncertainty is 1–2% in the optical filters, and around 10% in the F170 filter.

3. DIG in M33

The $H\alpha$ mosaic of M33 is discussed in detail in Greenawalt (1998). We briefly repeat the relevant results here. The diffuse fraction of M33 was found to be 40%, in good agreement with all other non-edge-on spirals studied so far. The Schmidt image reveals the DIG to be a complex network of filaments and arcs, superimposed upon a fainter, more diffuse background. As in other spirals, DIG is concentrated in regions of high star formation, and in the inner disk, but it is much more extended than the star forming regions, filling the disk with faint $H\alpha$ emission. Narrow-band imaging of the DIG in M33 (Greenawalt 1998) reveals that it shows the same spectral signature of enhanced [SII] seen in other galaxies.

4. $H\alpha$ –UIT Analysis

The FUV/ $H\alpha$ ratio in the DIG can constrain the source of ionization. For example, if the measured ratio in the DIG did not correspond to any reasonable average spectral type or population

of ionizing stars, we would conclude that the ionizing photons in the DIG are not produced locally. To perform this test we measured the FUV flux (L_{1520}) in the UIT image and the $H\alpha$ flux in the Schmidt image. For HII regions, we defined an aperture and a background annulus on the $H\alpha$ image, and then used the same aperture and annulus on the FUV image. For DIG, we measured the fluxes in $500 \text{ pc} \times 500 \text{ pc}$ square apertures (in the plane of the sky), with the HII regions masked out. The HII region mask was defined on the $H\alpha$ image and applied to both the $H\alpha$ and FUV images. This is slightly different from the approach taken in Hoopes & Walterbos (1997). In that paper the fluxes were measured in smaller apertures, leading to the possibility that in HII regions an aperture may miss the concentrated cluster of OB stars while still containing $H\alpha$ emission, leading to very high $H\alpha / L_{1520}$ ratios and thereby increasing the scatter in the distribution of ratios. Also in that paper no background was subtracted from the HII regions, contrary to the approach taken here. The background subtraction typically affects the $H\alpha$ flux of the HII regions by only 1–2%, but in the FUV image the contrast between HII regions and the field is not as high as in $H\alpha$, and the background subtraction can reduce the FUV flux by as much as 50%, and even more for faint HII regions.

We computed the number of ionizing photons (N_{Lyc}) from the $H\alpha$ luminosity, assuming ionization equilibrium and case B recombination (Osterbrock 1989) and neglecting absorption of ionizing photons by dust. The histograms in figure 2 show the resulting distribution of N_{Lyc}/L_{1520} ratios for the two environments. The histograms are shown sideways for comparison with models (see below). The observed ratios are shown; they have not been corrected for foreground or internal extinction. The N_{Lyc}/L_{1520} ratio in DIG is lower than that in HII regions. This fits a scenario in which the ionizing stars in the DIG are of later type than those in HII regions, since the later type stars would produce a lower ratio of ionizing to non-ionizing UV photons.

In figure 2 we compare the N_{Lyc}/L_{1520} ratios with models of evolving stellar populations. We used the Starburst99 evolutionary model to compute the ratio of ionizing photons to FUV flux (Leitherer *et al.* 1999). The model used a Salpeter (1995) initial mass function (IMF) with an upper mass cutoff of $120 M_{\odot}$. LMC-like ($Z=0.008$) metallicity models were calculated. The metallicity of M33 in the central region is about solar, but there is a steep gradient towards lower metallicity with distance from the center (Vílchez *et al.* 1988), so that overall M33 is subsolar in metallicity. Single burst and steady state models are presented. The reddening bars shown indicate the direction that the *models* would move if reddened by the given amount. Both the LMC (Howarth 1983) and Galactic (Cardelli, Clayton, & Mathis 1989) extinction laws are given, and the case of a foreground screen and a uniform mixture of dust and gas are shown for each extinction law. Massey *et al.* (1995b) found an average color excess of $E(B-V)=0.16$ in several fields of M33. The Galactic foreground produces a color excess of $E(B-V)=0.03\pm 0.02$ at this location (McClure & Racine 1969), and the rest is internal to M33. The extinction in the Massey *et al.* (1995b) fields ranges from $E(B-V)=0.09$ to 0.33. We also show reddened versions of each model. The steady state model, which represents the population expected outside of HII regions, was reddened by $E(B-V)=0.1$, while the single burst model, which represents the population in an HII region, was

reddened by $E(B-V)=0.2$, all using the LMC extinction law. The dashed line is reddened assuming a uniform mixture, and the dotted line is reddened assuming a foreground screen. Each reddened model also includes $E(B-V)=0.03$ of foreground Galactic reddening, using the Galactic extinction law.

The DIG distribution is consistent with an older burst population, or with a steady state, constant star formation model. The steady state model is probably a more accurate description of the stellar population in the DIG, but it is only an approximation. Figure 2 also shows the predictions of the steady state model using steeper IMF slopes than the usual Salpeter slope of $\alpha=-2.35$. Although the predicted ratios are below the observed ratio, with a reasonable amount of extinction the prediction for $\alpha=-3.0$ would match the observed DIG values well. This is interesting in light of the fact that Massey *et al.* (1995a) found a steeper IMF slope for OB stars in the field in the LMC and SMC. We will explore this issue further in section 6. The HII regions resemble a young burst population. The model values are dependent on the assumed IMF, and in small HII regions (which are the most numerous) that have low numbers of massive stars, the ionizing flux of a single O star may dominate the light from the UV emitting B stars. Figure 3 shows the same histograms along with the expected ratios from ionizing stars, taken from the CoStar stellar models (Schaerer & de Koter 1997). We show models using low metallicity ($Z=0.004$) and solar metallicity ($Z=0.020$), to cover the extreme values. Again the DIG ratio can be explained by later type ionizing stars.

The $N_{Ly\alpha}/L_{1520}$ ratio in the DIG can be explained with a local ionization model, where the ionizing population in the DIG is older than that in HII regions. However, the UIT analysis is far from conclusive. The ionizing photons which produce the $H\alpha$ emission seen in the DIG may be produced elsewhere and then leak into the DIG, as in the leaky HII regions explanation for the ionization of the DIG. In this case the models in figure 2 and 3 would not apply. To test this more conclusively, we need to find out whether the ionizing photons are produced locally. We investigate this further in the next section.

If the difference in the $FUV/H\alpha$ ratio between DIG and HII regions were due to higher extinction in the HII regions, at least 0.9 magnitudes A_V in excess of that in the DIG would be necessary to explain the result using a foreground screen model, and much higher for a uniform mixture. Greenawalt, Walterbos, & Braun (1997) found, on average, a 0.3 magnitude difference in extinction between HII regions and DIG in M31. Our stellar photometry (see the next section) indicates that there is on average little difference in the amount of extinction in the two environments. However, this is for only a very small part of the disk, so to be consistent with Greenawalt, Walterbos, & Braun (1997) we reddened the burst models more than the steady state models in figures 2 and 3.

5. HST Photometry

5.1. Spectral Classification of OB Stars

The most conclusive test of whether field stars can ionize the DIG would be to find the spectral types of all the OB stars outside of HII regions, add up the number of ionizing photons contributed by each star, and compare the total to that required by the $H\alpha$ luminosity of the DIG. Massey (1985) and Massey *et al.* (1995b) have shown that optical photometry is unable to distinguish between the different spectral types of ionizing stars, a distinction that must be made if accurate Lyman continuum luminosities are to be determined. This is because the peak of the Planck spectrum lies blueward of these filters for stars of 30,000 K or hotter, so optical filters sample the Rayleigh-Jeans portion of the spectrum which has a constant slope independent of temperature. Spectroscopy is the most reliable way to determine spectral types of massive stars, but obtaining spectroscopy of a large sample of field stars in M33 would require a prohibitive amount of telescope time. However, FUV photometry combined with optical photometry can be used to estimate spectral types of ionizing stars with reasonable accuracy. The F170W is closer to the peak of the Planck spectrum for temperatures above 30,000 K, providing an advantage over optical photometry alone.

The archival HST images cover DIG of varying brightness (see overlay of figure 1). However, they do not overlap any very luminous HII regions, only moderate and low-luminosity HII regions. This is a limitation of the data, and it prevents us from investigating whether the brightest HII regions are density-bounded. It should be noted that the HST images cover a much smaller area of the disk of M33 than the UIT image, so the focus of the analysis shifts here from a global to a local perspective. The HST pointings are all located in the inner disk of M33, within $10'$ from the nucleus, where the metallicity is close to solar (Vílchez *et al.* 1988). For this reason we assume solar metallicity when employing stellar models in the analysis of the WFPC2 images.

We put the $H\alpha$ image of M33 on the same grid as the WFPC2 frames, and then classified the stars in the WFPC2 images as being either in an HII region or in the field based on the $H\alpha$ surface brightness. An isophotal cut was used, but the level was adjusted to satisfactorily isolate the two environments based on their morphology. In the inner disk the cut level is as high as 200 pc cm^{-6} , while in the outer disk it is as low as 60 pc cm^{-6} . Individual HII regions were then picked from the masked image by eye. The rest of the image was counted as DIG. Only the Wide Field images were used, as there were no complete HII regions in the Planetary Camera images, and they do not cover a large enough area of DIG to analyze.

Holtzman *et al.* (1995) caution that the response curves of the main photometric filters used with WFPC2 (F336W, F439W, F555W), are sufficiently different from the groundbased analogs (UBV), that any reddening correction must be applied to the photometry in the HST filter system. Thus we derived reddening relations for the HST filter system used in this project, rather than transform the photometry to the groundbased system. We used the model stellar spectra of Lejeune,

Cuisinier, & Buser (1997), and reddened them according to both the Galactic extinction law (Cardelli, Clayton, & Mathis 1989) and the LMC law (Howarth 1983). We used the Lejeune, Cuisinier, & Buser (1997) model spectra rather than the CoStar models used below because the Lejeune *et al.* models extend to spectral types later than B0, allowing more of the unevolved main sequence to be used in determining the extinction. The reddened spectra were multiplied by the HST filter response curves to obtain the magnitude. The derived relations agree with those found in Holtzman *et al.* (1995), although the F170W relation was not given. We found that the LMC extinction law worked more satisfactorily than the Galactic law for reddening all bands to match the observed colors. As before, the reddening includes a correction for $E(B-V)=0.03$ foreground reddening using the Galactic extinction law, and any excess reddening using the LMC extinction law.

Figure 4 shows representative color-magnitude diagrams (CMDs) for HII regions and DIG regions in M33. Isochrones of ages 0 and 7×10^6 years are also shown. The isochrones were generated using the Geneva stellar evolution models (Schaerer *et al.* 1993). In order to put the isochrones in the STMAG system, for each stellar mass at each age we found the closest match in T_{eff} and $logg$ in the model stellar spectra of Lejeune, Cuisinier, & Buser (1997). The spectrum was then multiplied by the WFPC2 filter response curves to derive the observed magnitude. The isochrones are shown for reference only, they are not the best fit to the CMD. The purpose of these isochrones was to determine the extinction for each region. The amount of extinction needed to match the observed main sequence with the isochrone is taken as the average extinction for that region. The same was done for the remaining stars not in HII regions, which are field stars in the DIG. Using a single value for extinction in either environment is obviously an over-simplification, but it is the best solution for the available data. The average extinction found in HII regions was $E(B-V)=0.14$, and in DIG it was $E(B-V)=0.13$. We estimate that the extinction can be determined with this method with a $1-\sigma$ accuracy of $E(B-V) = \pm 0.02$.

We assigned spectral types based on the CoStar models of Schaerer & de Koter (1997). They provide spectral energy distributions for stars of mass 20, 25, 40, 60, 85, and $120 M_{\odot}$ at various ages in the Leitherer *et al.* (1996a) database. We used the solar metallicity ($Z=0.020$) models to match the metallicity where the HST pointings are located. We ran the model spectra through the HST filters, and linearly interpolated the magnitudes and other stellar properties (*e.g.* temperature, surface gravity, and ionizing photon luminosity) to the ages and masses between those given, to create a complete grid with $1 M_{\odot}$ mass resolution and 10^5 year time resolution. We then searched for the nearest match to the four magnitudes measured for each star. Thus for each star we go directly from the measured photometry to ionizing luminosity. The uncertainty in the ionizing luminosity is determined by the uncertainty in the photometry, ignoring uncertainty in the accuracy of the models, which is difficult to quantify.

We then inspected the color magnitude diagrams and the positions of the stars that were classified, noting any UV-bright stars that were not classified. In order to classify these stars, we adjusted the tolerance for the F555W magnitude, and if necessary for the F439W magnitude as

well. In most cases the tolerance was increased to $2\text{-}\sigma$, and in a few cases, $3\text{-}\sigma$. A small number of stars were in crowded regions and obviously had mismatched F555W and F439W magnitudes (crowding usually does not affect the UV magnitudes since fewer stars show up in the UV images), so we used only F170W and F336W magnitudes for classification. Most stars were matched within $1\text{-}\sigma$ of the four measured magnitudes.

We compared our photometric spectral types to previous spectroscopic spectral types to assess the accuracy of the photometric technique. We looked for overlapping stars in Massey *et al.* (1995b) and Massey *et al.* (1996), finding only two stars that overlap, both in Massey *et al.* (1996). The reason is that our technique only assigns spectral types to B0 stars and earlier, so while many B stars overlapped, we did not assign spectral types to them, so they could not be used for comparison. The properties that the photometric technique assigned to the two stars are shown in table 2, along with the properties of the spectral type assigned by Massey *et al.* (1996). These properties are taken from Vacca, Garmany, & Shull (1996). The properties that the photometric technique assigned to both stars match reasonably well with the properties expected for stars of the correct spectral type. It should be noted that UIT104 is a Wolf-Rayet star, and might not be expected to match the properties of an O9Ia star. Nevertheless, the agreement gives us reason to believe that the photometrically determined spectral types agree with those determined spectroscopically, to within about a spectral type.

5.2. Comparison of Predicted and Observed $H\alpha$ Luminosity

For each HII region we summed the predicted ionizing luminosity of all the stars included in the region. The predicted ionizing luminosity in the DIG was the cumulative luminosity of stars not included in an HII region. Each chip of each WFPC2 pointing was considered separately. We converted the predicted ionizing luminosity to a predicted $H\alpha$ luminosity $L_{H\alpha}$, assuming that all ionizing photons result in an ionization (*i.e.* no dust absorption) and case B recombination. The predicted $L_{H\alpha}$ was then compared to the observed $L_{H\alpha}$. We measured the observed $L_{H\alpha}$ from the $H\alpha$ image (figure 1). The boundaries of the HII regions were determined on the masked image, and a background correction for the surrounding DIG was subtracted. HII regions which were not completely contained within the HST pointing were not considered. The $L_{H\alpha}$ for DIG was the sum of all the luminosity not in an HII region. The luminosities were corrected for extinction using the estimates of $E(B-V)$ from the color-magnitude diagrams.

In figure 5 we compare the predicted $L_{H\alpha}$, based on the ionizing luminosity of the stars present, with the observed $L_{H\alpha}$ from the $H\alpha$ image for both HII regions and DIG. The errors reflect a combination of uncertainty in photometry and in extinction. The effect of photometric errors on the ionizing luminosity was calculated by determining for each star the model with the highest $N_{Ly\alpha}$ and the model with the lowest $N_{Ly\alpha}$ that still matched within the photometric errors. When the best match luminosities were added for all stars in the region, the range found for each star was added in quadrature. The effects of uncertainty in extinction were quantified by varying

the correction by $E(B-V)=\pm 0.02$, and again calculating the total ionizing luminosity of the stars in a region. These two uncertainties were added together in quadrature to produce the error bars shown in figure 5.

Qualitatively, we find that the measured $L_{H\alpha}$ for both HII regions and DIG agree well with the predicted luminosities. There is considerable scatter, but given the uncertainties in stellar models, extinction in the UV, and spectral classification without the use of spectra, the agreement is encouraging. The observed $L_{H\alpha}$ is corrected for extinction, but the predicted $L_{H\alpha}$ may be an overestimate since we ignore the possibility of ionizing photons being absorbed by dust. To correct for this we would have to know how much of the ionizing luminosity of a star is absorbed by dust. McKee & Williams (1997) estimate the fraction of dust absorbed in Galactic HII regions to be about 25%, perhaps slightly lower for smaller HII regions such as those we consider here.

Figure 5 shows that while the mean ratio is close to unity, some HII regions are under-predicted or over predicted. This is an indication that predictions for individual regions are not reliable, but that the average for all the regions is better. Thus a comparison of the average values for DIG and HII regions is more illuminating than individual regions. The average ratio of predicted to required $L_{H\alpha}$ are given in table 3. For HII regions the predictions are consistent with the observed $L_{H\alpha}$. For DIG regions there are not enough ionizing photons emitted by field stars to account for all of the observed $H\alpha$ emission, but there are enough to provide a significant fraction of the ionization, about 40%.

To test the idea that FUV information is necessary to estimate the spectral types of ionizing stars, we re-classified the ionizing stars using only the F336W, F439W, and F555W magnitudes. The results are given in table 3. The predicted $L_{H\alpha}$ is higher, and most HII regions are over-predicted, leading to a large excess of ionizing photons. If the FUV information had been ignored in the initial classification, many non-ionizing stars would have been classified as ionizing stars, leading to a further excess. The FUV information is crucial to accurately predict ionizing fluxes, and optical information alone will lead to a severe over prediction of ionizing fluxes of OB stars. This test underscores the difficulty of drawing conclusions about OB stars based on optical photometry (Patel & Wilson 1995, see also O’Dell, Hodge, & Kennicutt 1999). This may account for the discrepancy in the fraction of OB stars found outside of HII regions. We identified 116 ionizing stars in the five WFPC fields. Of these, 27% (31 stars) were in the DIG, lower than the $\sim 50\%$ found by Patel & Wilson (1995). However, it is important to remember that we can only investigate a small fraction of the disk of M33 with the present HST data.

5.3. Characteristics of the HII Regions

Oey & Kennicutt (1997) found that 2 out of 14 HII regions in the LMC are leaking a sizeable number of ionizing photons. These two HII regions both have a ring-like morphology, leading to the question of whether HII morphology is correlated the amount of leakage. This is an important

question in light of suggestions that ionizing photons escaping from superbubbles may be an important ionization source (Dove, Shull, & Ferrara 2000). Softening of the spectrum by re-radiation of ionizing photons through chimney walls may explain the low HeI measurements (Norman 1991). We classified the HII regions in the HST field based on their morphology in the H α image, in order to look for trends in the amount of leakage with morphology. Figure 6 shows this comparison. The HII regions are either compact, meaning center brightened and obviously discrete, or diffuse, which includes rings, filaments, and faint tenuous HII regions (the ring-like HII regions are shown as double open circles). It appears that compact and diffuse HII regions are equally likely to be density-bounded.

In figure 6 we also see that there is no significant trend for leakiness with $L_{H\alpha}$. It is very important to remember that the brightest HII regions in M33 were not imaged in the HST data, and only a few in our sample are more luminous than 10^{38} erg s $^{-1}$ (corrected for internal extinction). Thus we cannot address the issue of whether the most luminous HII regions are density-bounded (Beckman *et al.* 2000). It is still interesting, however, that the two brightest HII regions in M33, NGC 604 (González Delgado & Pérez 2000) and NGC 595 (Malamuth, Waller, & Parker 1996), appear to be radiation-bounded. In a future paper we will investigate the brightest HII regions in M33.

6. UIT - HST Comparison

The WFPC2 images resolve stars above a limiting magnitude, which in the F170W filter corresponds to about a B0 star. The UIT image measures all of the FUV surface brightness of the entire population of UV emitting stars. The UIT image sensitivity extends to 50-100 Myr old populations (O’Connell 1997), which corresponds to B and early A type stars, so a comparison of the UV flux measured by HST and UIT thus compares the stars of spectral type B0 and earlier to the entire OBA population. This is an age dependent ratio which can be modeled, and may be used to further characterize the stellar population in both HII regions and DIG. The attractive feature of this comparison is that it is largely independent of extinction, as both filters cover a similar range of wavelengths (however extinction must still be incorporated, see below).

We have performed this comparison for the HII regions and DIG on the HST fields. The FUV flux from the UIT image was measured using the same apertures used to measure the H α flux. We then summed up the FUV flux of the stars brighter than a magnitude limit in the same regions in the HST images. In order to keep a consistent limiting magnitude, we reddened the F170W magnitude of a B0 star ($M_{F170W}=16.92$) using the extinction found from the CMDs and used throughout this analysis, and summed the flux from all stars brighter than this magnitude. This is the point where extinction becomes important in this comparison, the determination of the cutoff magnitude in the HST images. The relationship between flux and magnitude in the STMAG system is given by

$$M_{F170W} = -2.5\log(F_{\lambda}) - 21.1 \quad (1)$$

(Holtzman *et al.* 1995). The flux was determined from the magnitudes *without* correcting for extinction, as the UIT flux is also uncorrected. The extinction is only used to determine the cutoff magnitude which corresponds to a B0 star.

A histogram of the ratios is shown in figure 7. The histogram shows a difference between the two populations, with DIG having a lower ratio of HST to UIT flux. This is expected if the DIG is ionized by an older population, with fewer stars earlier than B0 relative the number of stars later than B0. Also shown on the plot are models of the evolution of this ratio through time, constructed using Starburst99 (Leitherer *et al.* 1999). The UIT flux was modeled as an evolving population with a mass range from 1 to 120 M_{\odot} , a Salpeter (1995) IMF, and solar metallicity. In order to simulate the populations seen in the HST FUV images, we needed to include flux only from stars with $M \geq 20M_{\odot}$, as this corresponds to the limiting spectral type of B0 in the HST images. To do this we ran the models again, except that mass range was 20 to 120 M_{\odot} , and the total mass was scaled down by 0.2 (so that the total mass, including stars with $M \leq 20M_{\odot}$, was $10^6 M_{\odot}$, as it was for the UIT simulation). This approach is simplistic, but provides a first-order model for comparison with the observations. As expected, the ratio of HST to UIT flux in the single burst model generally decreases as time passes and the most massive stars die. The observed ratios for HII regions match well with the predicted values for single burst populations. An older burst model reproduces the DIG ratios reasonably well.

We also ran steady state models as described above, but the resulting ratio did not agree well with the observed ratio for the DIG, contrary to the analysis in figure 2. The disagreement may indicate that if the steady state model is an accurate description of the stellar population in the DIG, the parameters used for the HII region stars may not apply to the field stars. Specifically, Massey *et al.* (1995a) derived the IMF for field stars in the LMC and SMC, and found a slope ranging from $\alpha = -4.7$ to -5.1 (in the notation where the Salpeter IMF slope α is -2.35). We ran models using IMF slopes for massive stars ($M \geq 20M_{\odot}$) of $\alpha = -3.5, -3$, and the standard Salpeter slope of -2.35 , while keeping the slope for less massive stars at $\alpha = -2.35$. The observed HST/UIT flux ratio agrees much better with the models using a steeper slope of $\alpha = -3$ than the Salpeter slope. This supports the conclusions of Massey *et al.* (1995a) regarding the IMF slope for field OB stars. The observed ratios suggest that the IMF slope for field OB stars in M33 is not as steep as that in the LMC and SMC, but is still steeper than the IMF in HII regions.

It should be noted that the Starburst99 models are intended for starburst regions, *i.e.* regions with a large number of stars. Most of the HII regions we are investigating do not fit into this category, so the model cannot be expected to accurately predict the observed ratio. The main problem is that with small numbers of massive stars, the IMF is not well sampled. This may be the reason behind the spread in the observed distribution of HST/UIT ratios, and also might explain why some HII regions have ratios too high to be explained by the models. However, the predicted ratio agrees with the majority of HII regions, which suggests that these deviations average out for a large number of HII regions. Also note that the two filters are not identical, and this is probably the reason some of the HII regions have $HST/UIT > 1$.

7. Discussion

Our most important result is that the OB stars outside of HII regions can account for 40% of the ionization of the DIG in M33. There are several points to keep in mind. One is the scale we are investigating, which is constrained by the size of the Wide Field chips of WFPC2, 325 pc across each chip. This means we are implicitly assuming that stars (field stars in particular) do not have an influence at distances greater than this, or that the number of photons escaping the image is balanced by the number of photons coming in from outside the image. In a uniform medium with $n=0.2 \text{ cm}^{-3}$, which is the density found for the DIG in the Galaxy, the Strömgren sphere of an O3V star has a diameter of about 770 pc (Osterbrock 1989, using the stellar ionizing flux in Vacca *et al.* 1996). However there are few of these stars outside of HII regions. One chip can completely contain the Strömgren sphere of an O8V star, and a B0V star ionizes a region about 170pc across. The density in the DIG in the inner regions of M33 may be higher than the density measured in the solar neighborhood, which would tend to make the ionized regions smaller. We cannot account for neighboring HII regions or ionizing stars outside of the WFPC2 field of view.

Another point to consider is the many uncertainties dealt with in this analysis. When working in the UV extinction is always a prime concern, and small changes in the adopted extinction, or in the extinction law, can cause large changes in the ionizing luminosity. When dealing with individual stars in external galaxies, crowding can often be a concern. The stars visible in the F170W filter are rarely crowded, but of course crowding may be present but not detectable, as in the case of binaries. Crowding may also be a more severe problem for OB associations in HII regions than for the more sparsely distributed stars in the DIG. Another source of uncertainty stems from the stellar atmosphere models which we use to assign Lyman continuum luminosities. The stellar models give excellent agreement for the non-ionizing spectrum of massive stars, but the ionizing spectrum is difficult to test without making assumptions. We have tried to be as conservative as possible in every aspect of this analysis. Given these uncertainties, it is remarkable that we find such good agreement between the predicted and observed $L_{H\alpha}$. This gives us confidence in the stellar models, and it also suggests that any mistakes we are making regarding the extinction and spectral classification are relatively small. It also suggests that we are detecting most, if not all, of the ionizing stars.

Without placing trust in the absolute accuracy of the predicted ionizing fluxes, it is possible to draw conclusions by comparing our predictions for DIG and HII regions. This comparison relies on the assumption that any errors in the prediction for the DIG will also be made for HII regions. The ratio of $N_{Ly\alpha}/L_{H\alpha}$ is lower in the DIG than in HII regions, indicating that some leakage is necessary to explain the DIG. However, the difference is not so great that field stars can be neglected as a source of ionization. The $N_{Ly\alpha}/L_{H\alpha}$ in the DIG is about 37% of the ratio in HII regions. If we normalize the $N_{Ly\alpha}/L_{H\alpha}$ to 100% in HII regions, this relative approach would suggest that field stars can ionize at least 37% of the DIG, well within the uncertainty of our absolute determination.

In the regions covered in the WFPC2 pointings, the fraction of the *total* $H\alpha$ luminosity that

comes from the DIG is 40%, which is also the diffuse fraction of the entire galaxy. In the five fields analyzed here, on average the field stars can account for $40\% \pm 12\%$ of the ionization of the DIG (it is a potentially confusing coincidence that these two numbers are the same). This implies that only 30% of the ionizing photons emitted in HII regions need to escape to account for the remaining DIG, or put differently, the predicted $L_{H\alpha}$ in HII regions should be 143% of the observed $L_{H\alpha}$ in HII regions. The average ratio of predicted to observed $L_{H\alpha}$ for HII regions is $107\% \pm 26\%$, so the amount of excess ionizing photons is not enough to explain all of the remaining DIG, with the maximum within the uncertainty being 133%. Simply adding up the observed and predicted $L_{H\alpha}$, we find that, within the uncertainty, 98% of the total observed $L_{H\alpha}$ (DIG+HII) can be explained by field stars plus leakage (taking the maximum predicted $N_{Ly\alpha}$ within the uncertainty). Also keep in mind that other processes may play some role in ionizing the DIG, such as turbulent mixing layers (Slavin, Shull, & Begelman 1993) and shock ionization. Most likely a combination of these processes, plus photons leaking from HII regions, ionize the rest of the DIG.

There is also the possibility that a fraction of the ionizing photons are absorbed by dust. McKee & Williams (1997) found that about 25% of the ionizing photons emitted by stars within HII regions are absorbed by dust. If this is the case, we then predict only 80% of the ionizing photons necessary to explain the $L_{H\alpha}$ of the HII regions. Since there is not even enough to explain the $L_{H\alpha}$ from HII regions, we cannot then explain the remaining DIG ionization with leaky HII regions. However, since we know that the HII regions are ionized by the stars within, the discrepancy might be explained by a systematic error in determining the spectral types and ionizing luminosities from the photometry. In this case we could then scale the predicted HII region luminosity up to 100%, and scale up the predicted DIG luminosity accordingly to perform a relative comparison. We could not address the question of whether any excess ionizing luminosity from stars in HII regions exists. If an equal fraction of the ionizing photons emitted by field OB stars is absorbed by dust, the results of this paper would not be greatly affected.

Taking the maximum predicted $N_{Ly\alpha}$ within the uncertainty, we find that there are no ionizing photons from stars left over to escape the galaxy altogether. Of course this depends on the contribution of other ionization sources to the DIG. If 20% of the DIG is ionized by another source, there can be as much as 4% of the stellar ionizing photons left over to escape the galaxy, within the error bars. The uncertainty in these numbers is such that we cannot place much weight on this limit. However, it is in agreement with Leitherer *et al.* (1995), who found that less than 3% of the ionizing photons escape from four starburst galaxies observed with HUT, although Hurwitz, Jelinsky, & Dixon (1997) suggest that the fraction could be as high as 57% for one of the galaxies by allowing for absorption by undetected components of the ISM. Deharveng *et al.* (1997) also find very little leakage, less than 1%. We must also remember that we are restricted to relatively small regions (about 650pc across), and are really covering only a small fraction of the disk of M33. We have no way of knowing whether excess photons emitted by stars in the image actually escape the galaxy, or simply ionize gas outside of the image. Similarly, there may be photons from outside of the image ionizing gas in the image.

Note that leaky HII regions can provide less than 60% of the ionization of the DIG in the regions of M33 studied here. This is in disagreement with the results of Oey & Kennicutt (1997), who found that the Lyman continuum escaping from HII regions could very likely account for all of the DIG emission in the LMC. This may point to a difference between the DIG in irregular galaxies and spirals. Martin & Kennicutt (1997) found that Helium is completely ionized in the DIG in several irregular galaxies, indicating ionization by very massive stars, type O7 or hotter. They concluded that density-bounded HII regions are the dominant source of ionization in those galaxies. A difference in the ionization source might explain the lower HeI 5876 Å/H α seen in some spirals (Reynolds & Tufte 1995; Rand 1997).

The field OB stars in M33 appear to have a steeper IMF than OB stars in HII regions, confirming the results of Massey *et al.* (1995a) for field OB stars in the LMC and SMC. The slope which best fits our observations is not as steep as that found in the LMC and SMC, but it is still different from that found in HII regions. The difference may imply a different formation mechanism for field stars, but does not necessarily mean that they form in the field. Field OB stars may have formed in an HII region and then drifted out of the dense cloud, or they may be the remnants of an OB association after the surrounding gas has dissipated through the actions of SNe and stellar winds. In either case, lower mass OB stars are more likely to become field stars, as they have longer lives and thus can drift farther, or live long enough to outlast the HII region. The result would be a steeper mass function for field OB stars, because the youngest and most massive stars are still associated with HII regions. In this case the varying IMF is used to simulate a steeper *mass function* for stars in the field, and it is not necessary that they have a different *initial* mass function. The steeper IMF merely represents the fact that the most massive HII region stars have a smaller chance of becoming field stars due to their short lifetimes. However, Massey *et al.* (1995a) carefully corrected for stars which may have drifted out of HII regions, and found stars as massive as 85 M $_{\odot}$ in the field. It is difficult to explain how a star this massive became a field star if it did not form in the field.

We thank the anonymous referee for a very careful reading of the manuscript and comments which improved the presentation of our results. We are grateful to Bruce Greenawalt for obtaining the H α data, and to Richard Rand for the use of his narrow band filters. The archival UIT image was obtained through the NASA Data Archive and Distribution Service. We would like to acknowledge the UIT project for making their data available. The availability of the Starburst99 models of C. Leitherer and collaborators is greatly appreciated. This research benefitted from helpful discussions with Jon Holtzman, Salman Hameed, Bruce Greenawalt, David Thilker, Nichole King, and Vanessa Galarza. Support for this work was provided by NASA through grant number AR07645.01-96A from the Space Telescope Science Institute, by NASA grant NAG5-2426, a Cottrell Scholar Award from Research Corporation, and by the NSF through grant AST-9617014. CGH was supported by a grant from the New Mexico Space Grant Consortium.

REFERENCES

- Beckman, J. E., Rozas, M., Zurita, A., Watson, R. A., & Knapen, J. H. 2000, *AJ*, 119, 2728
- Cardelli, J. A., Clayton, G. C., & Mathis, J. S. 1989, *ApJ*, 345, 245
- Chandar, R., Bianchi, L., & Ford, H. C. 1999, *ApJS*, 122, 431
- Deharveng, J. -M., Faiesse, S., Milliard, B., & Le Brun, V. 1997. *A&A*, 325, 1259
- Dettmar, R. -J. 1990, *A&A*, 232, L15
- Domgörgen, H. & Mathis, J. S. 1994, *ApJ*, 428, 647
- Dove, J. B., Shull, M. J., & Ferarra, A, 2000, *ApJ*, 531, 846
- Ferguson, A. M. N., Wyse, R. F. G., Gallagher, J. S., Hunter, D. A. 1996, *AJ*, 111, 2265
- Freedman, W. L., Wilson, C. D., & Madore, B. F. 1991, *ApJ*, 372, 45
- Garmany, C. D., Conti, P. S., & Chiosi, C. 1982, *ApJ*, 263, 777
- González Delgado, R. M. & Pérez, E. 2000, *MNRAS*, preprint (astro-ph 0003067)
- Gordon, S. M., Kirshner, R. P., Long, K. S., Blair, W. P., Duric, N., Smith, R. C. 1998, *ApJS*, 117, 89
- Greenawalt, B. 1998, Ph.D. Thesis, New Mexico State University
- Greenawalt, B., Walterbos, R. A. M., & Braun, R. 1997, *ApJ*, 483, 666
- Greenawalt, B., Walterbos, R. A. M., Thilker, D. A., & Hoopes, C. G. 1998, *ApJ*, 506, 135
- Haffner, L. M., Reynolds, R. J., & Tufte, S. L. 1999, *ApJ*, 523, 223
- Hester, J. J. & Kulkarni, S. A 1990, in *The Interstellar Medium in External Galaxies*, ed. D. Hollenbach & H. Thronson (NASA CP-3038), 288
- Holtzman, J. A., et al. 1995, *PASP*, 107, 156
- Hoopes, C. G. & Walterbos, R. A. M. 1997, in *The Ultraviolet Universe at Low and High Redshift: Probing the Progress of Galaxy Evolution*, ed. W. H. Waller, M. N. Fanelli, J. E. Hollis, & A. C. Danks (New York: AIP), 94
- Hoopes, C. G., Walterbos, R. A. M., & Greenawalt, B. 1996, *AJ*, 112, 1429
- Hoopes, C. G., Walterbos, R. A. M., & Rand, R. J. 1999, *ApJ*, 522, 669
- Howarth, I. D. 1983, *MNRAS*, 203, 301

- Humphreys, R. M. & Sandage, A. 1980, ApJ, 44, 319
- Hurwitz, M., Jelinsky, P., & Dixon, W. V. D. 1997, ApJ, 481, L31
- Landsman, W. B., Roberts, M. S., Bohlin, R. C., O’Connell, R. W., Smith, A. M., & Stecher, T. P. 1992, ApJ, 401, L83
- Leitherer, C., Ferguson, H. C., Heckman, T. M., & Lowenthal, J. D. 1995, ApJ, 454, L19
- Leitherer, C. *et al.* , 1996a, PASP, 108, 996
- Leitherer, C., Schaerer, D. Goldader, J. D., GonzálezDelgado, R. M., Robert, C., Foo Kune, D., de Mello, D. F., Devost, D., & Heckman, T. M. 1999, ApJS, 123, 3
- Leitherer, C., Vacca, W. D., Conti, P. S., Filippenko, A. V., Robert, C., & Sargent, W. L. W. 1996b, ApJ, 465, 717
- Lejeune, T., Cuisinier, F., & Buser, R. 1997, A&AS, 125, 229
- Malamuth, E. M., Waller, W. H., & Parker, J. W. 1996, AJ, 111, 1128
- Martin, C. L. & Kennicutt, R. C. 1997, ApJ, 483, 698
- Massey, P. 1985, PASP, 97, 5
- Massey, P., Armandroff, T. E., Pyke, R., Patel, K., & Wilson, C. D. 1995b, AJ, 110, 2715
- Massey, P., Bianchi, L., Hutchings, J. B., and Stecher, T. P. 1996, ApJ, 469, 629
- Massey, P., Lang, C. C., DeGioia-Eastwood, K., & Garmany, C. D. 1995a, ApJ, 438,188
- McClure, R. D. & Racine, R. 1969, AJ, 74, 1000
- McKee, C. F. & Williams, J. P. 1997, ApJ, 476, 144
- Norman, C. A. 1991, in The Interstellar Disk-Halo Connection in Galaxies, IAU Symposium No. 144, edited by H. Bloemen (Dordrecht:Kluwer), 337
- O’Connell, R. W. 1997, in The Ultraviolet Universe at Low and High Redshift: Probing the Progress of Galaxy Evolution, ed. W. H. Waller, M. N. Fanelli, J. E. Hollis, & A. C. Danks (New York: AIP), 11
- O’Dell, C. R., Hodge, P. W., & Kennicutt, R. C. 1999, PASP, 111, 1382
- Oey, M. S. & Kennicutt, R. C. 1997, MNRAS, 291, 827
- Osterbrock, D. E. 1989, Astrophysics of Gaseous Nebulae and Active Galactic Nuclei (Mill Valley: University Science Books)

- Patel, K., & Wilson, C. D. 1995, *ApJ*, 451, 607
- Pildis, R. A., Bregman, J. N., & Schombert, J. M. 1994, *ApJ*, 427, 160
- Rand, R. J. 1996, *ApJ*, 462, 712
- Rand, R. J. 1997, *ApJ*, 474, 129
- Rand, R. J. 1998, *ApJ*, 501, 137
- Rand, R. J., Kulkarni, S. R., & Hester J. J. 1990, *ApJ*, 396, 97
- Reynolds, R. J, 1984 *ApJ*, 282, 191
- Reynolds, R. J, 1985 *ApJ*, 298, L27
- Reynolds, R. J. 1991, in *The Interstellar Disk-Halo Connection in Galaxies*, IAU Symposium No. 144, edited by H. Bloemen (Dordrecht:Kluwer), 67
- Reynolds, R. J. & Tufte, S. L. 1995, *ApJ*, 439, L17
- Rubin, R. H., Simpson, J. P., Haas, M. R., & Erickson, E. F. 1991, *ApJ*, 374, 564
- Salpeter, E. E. 1955, *ApJ*, 121, 161
- Schaerer, D. & de Koter, A. 1997, *A&A*, 322, 598
- Schaerer D., Meynet G., Maeder A., Schaller G., 1993, *A&AS* 98, 523
- Slavin, J. D., Shull, J. M., & Begelman, M. C. 1993, *ApJ*, 407, 83
- Stecher, T., *et al.* 1992, *ApJ*, 359, L1
- Stecher, T., *et al.* 1997, *PASP*, 109, 584
- Torres-Peimbert, S., Lazcano-Araujo, A., & Peimbert, M. 1974, *ApJ*, 191, 401
- Vacca, W. D., Garmany, C. D., & Shull, J. M. 1996, *ApJ*, 460, 914
- Vílchez, J. M., Pagel, B. E. J., Diaz, A. I., Terlevich, E., & Edmunds, M. G. 1988, *MNRAS*, 235, 633
- Walterbos, R. A. M., & Braun, R. 1994, *ApJ*, 431, 156
- Walterbos, R. A. M., & Braun, R. 1996, in *ASP Conf. Proc. 106, The Minnesota Lectures on Extragalactic Neutral Hydrogen*, ed. E. D. Skillman (San Francisco:ASP), 1
- Wang, J., Heckman, T. M., & Lehnert, M. D. 1997, *ApJ*, 491, 114
- Wang, J., Heckman, T. M., & Lehnert, M. D. 1999, *ApJ*, 515, 97

Webber, W. R. 1998, ApJ, 506, 329

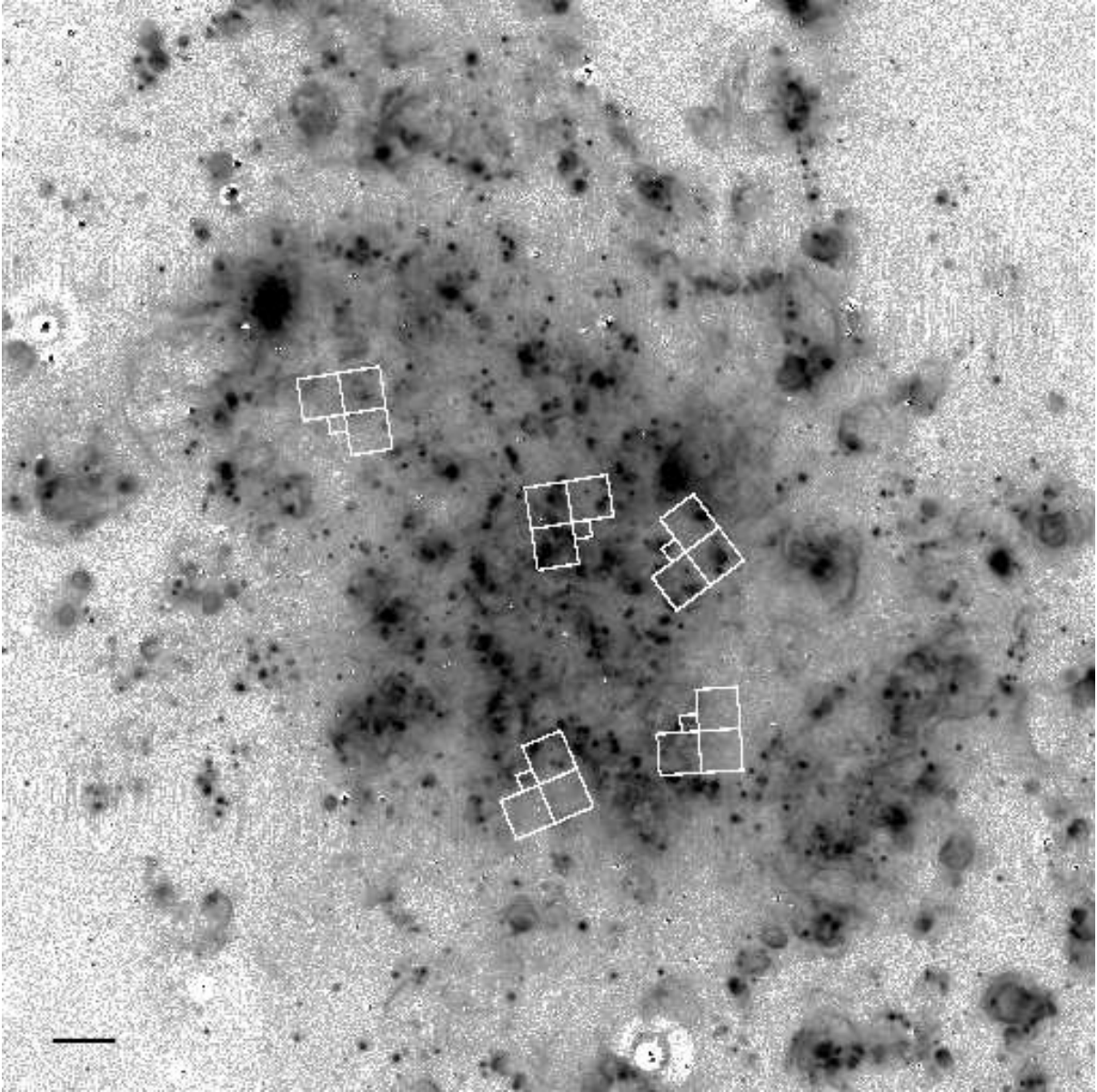


Fig. 1.— Continuum-subtracted $H\alpha$ image of M33, taken with the Burrell Schmidt. North is up and east is to the left. Only the central $30'$ of M33 are shown in this figure. The bar in the lower left corner represents $2'$ ($=489$ pc at the assumed distance of 0.84 Mpc to M33). The overlay shows the locations of the archival HST WFPC2 data used for this project.

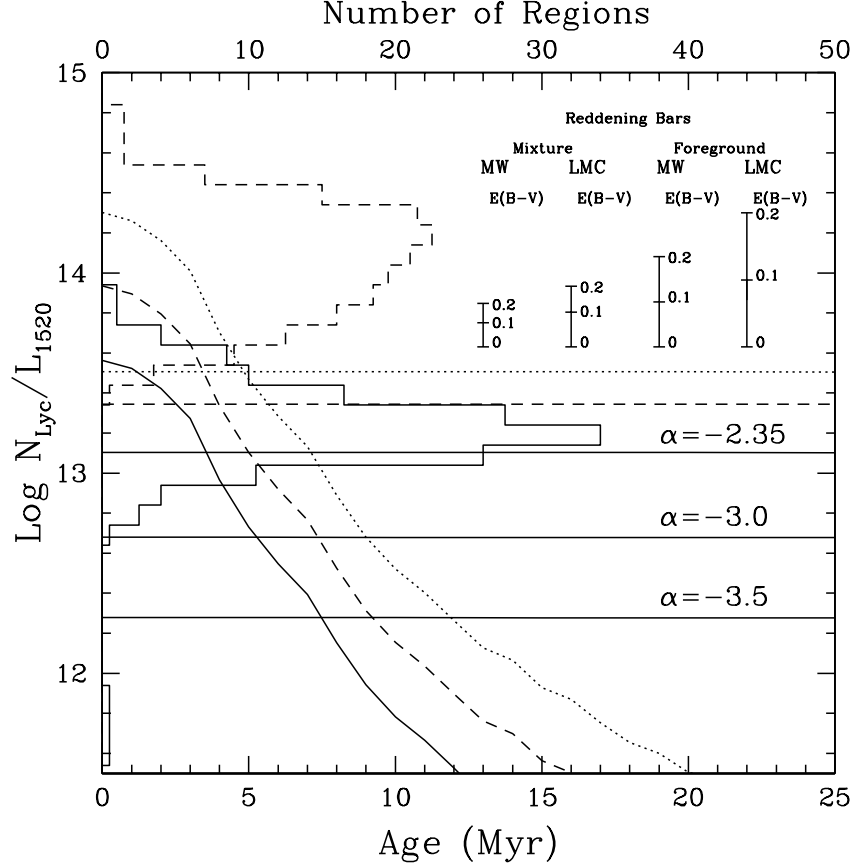


Fig. 2.— Ratio of the number of ionizing photons (N_{Lyc}) to the FUV luminosity from the UIT B1 band image (L_{1520}) for DIG (solid histogram) and HII regions (dashed histogram). The histograms have not been corrected for reddening. The models are computed from the Starburst99 evolution code (Leitherer *et al.* 1999), with an upper mass cutoff of $100 M_{\odot}$ and LMC ($Z=0.008$) metallicity. Two models are shown, a single burst (falling lines) and a steady state model with a constant star formation rate (straight lines). The dashed lines show the models reddened assuming a uniform mixture of gas and dust, and the dotted line shows the models reddened assuming a foreground screen of dust. The burst models were reddened by $E(B-V)=0.2$ internal extinction using the LMC extinction law (Howarth 1983), plus $E(B-V)=0.03$ Galactic foreground extinction. The steady state models were reddened by $E(B-V)=0.1$ internal extinction using the LMC extinction law, plus $E(B-V)=0.03$ Galactic foreground extinction. The effects of reddening on the models are shown in the reddening bars at the top right. Predictions for the steady state model using steeper IMF slopes are also shown, but without reddened versions.

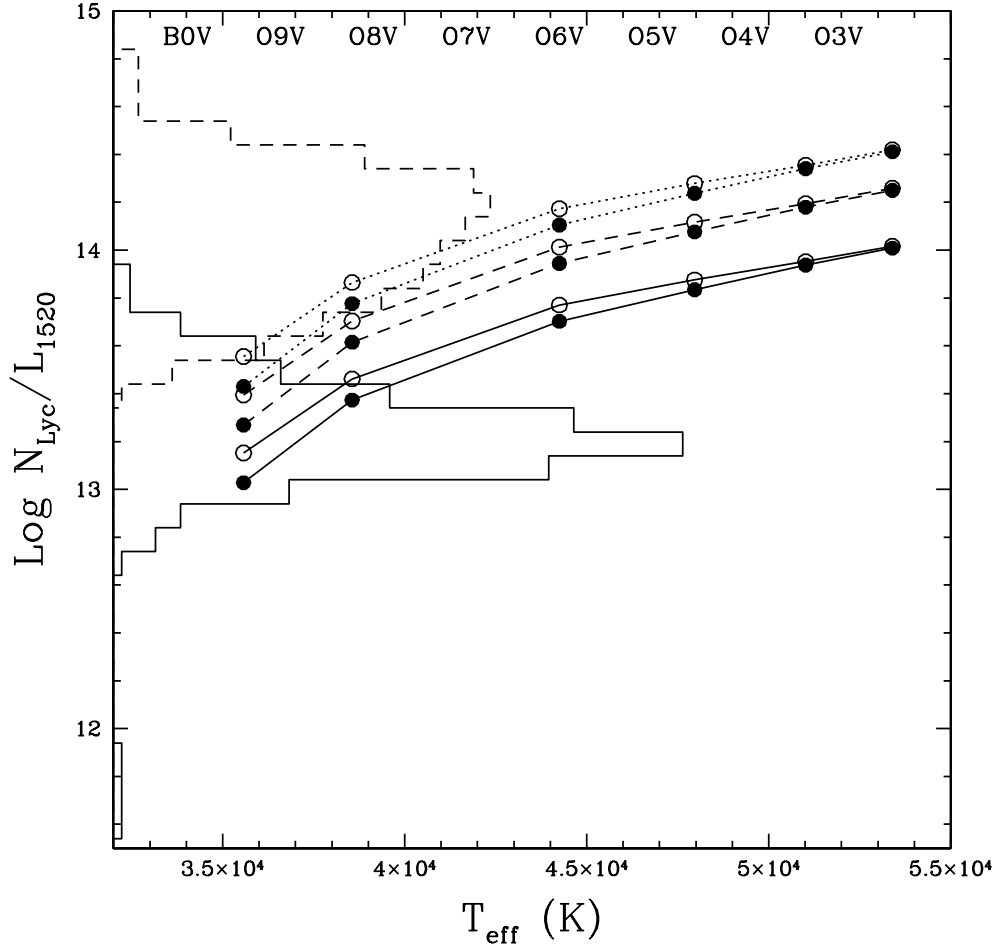


Fig. 3.— Ratio of the number of ionizing photons (N_{Lyc}) to the FUV luminosity from the UIT B1 band image (L_{1520}) for DIG and HII regions (same as figure 2), compared to model stellar atmospheres. The theoretical ratios were computed using the CoStar stellar atmosphere models of Schaerer & de Koter (1997). The open circles are for models with metallicity $Z=0.004$, and the filled circles are models with $Z=0.020$. The dashed line represents model stars that have been reddened by $E(B-V)=0.1$ using the LMC extinction law and uniform mixture model, and the dotted line indicates models that have been reddened by $E(B-V)=0.1$ using the LMC extinction law and a foreground screen model. Both of the reddened models also have been reddened by the $E(B-V)=0.03$ Galactic foreground.

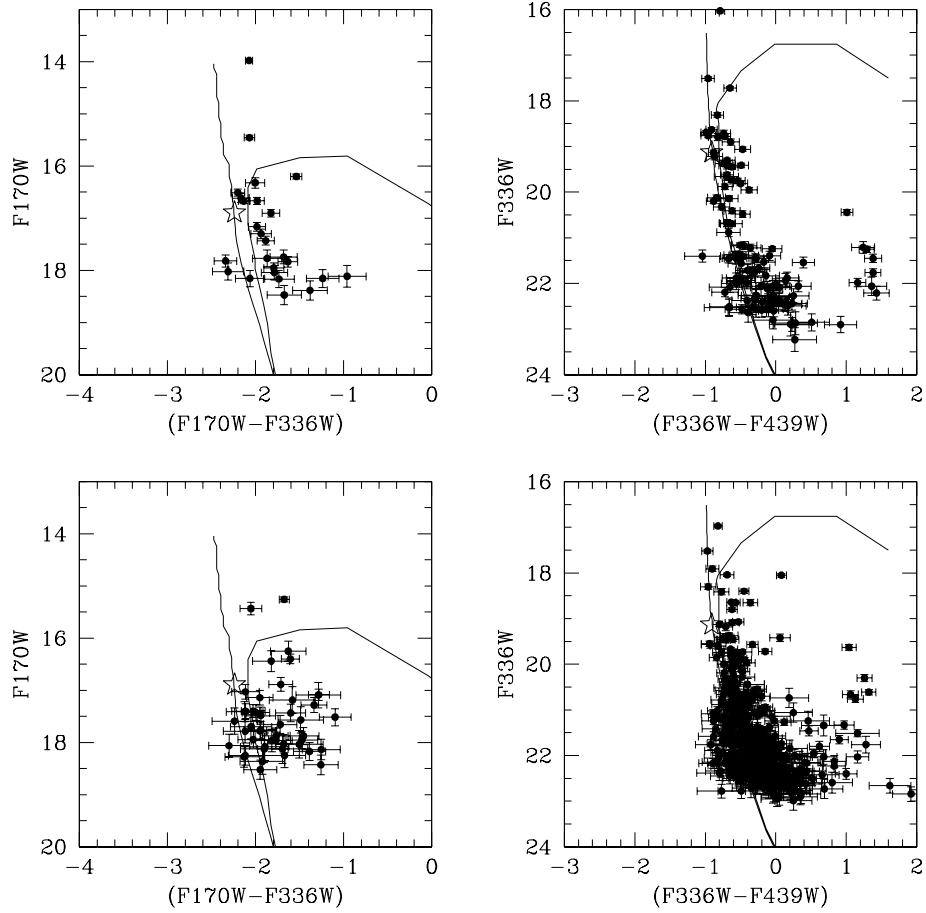


Fig. 4.— Examples of color-magnitude diagrams from the WFPC2 photometry. An HII region is shown in the top two panels, and a region of DIG is shown in the bottom two panels. Isochrones are from the Geneva group (Schaerer *et al.* 1993) and have been converted to the HST filter system, and show ages of 0 Myr and 7 Myr. They are shown as a reference point only; they are not the best match to the age of the population. The stellar magnitudes have been corrected for reddening using the LMC extinction law. The amount of reddening was found by moving the main sequence to fit the isochrones. The 5 pointed symbol shows the position of a B0V star.

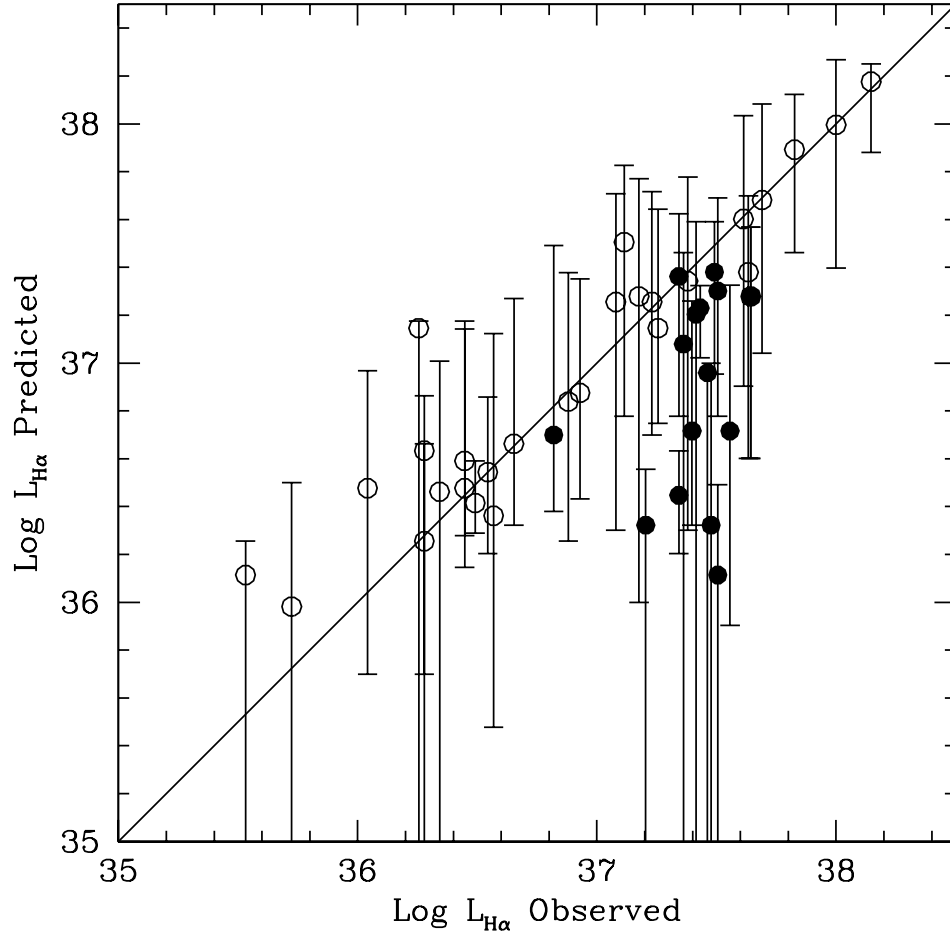


Fig. 5.— Comparison of predicted to observed H α luminosity, based on the spectral types of the stars observed in each region. HII regions are shown as open circles and DIG regions are shown as filled circles. The error bars are a combination of uncertainty in the spectral classification due to photometric errors and uncertainty due to extinction. In some regions the lower errorbar equals zero ionizing photons.

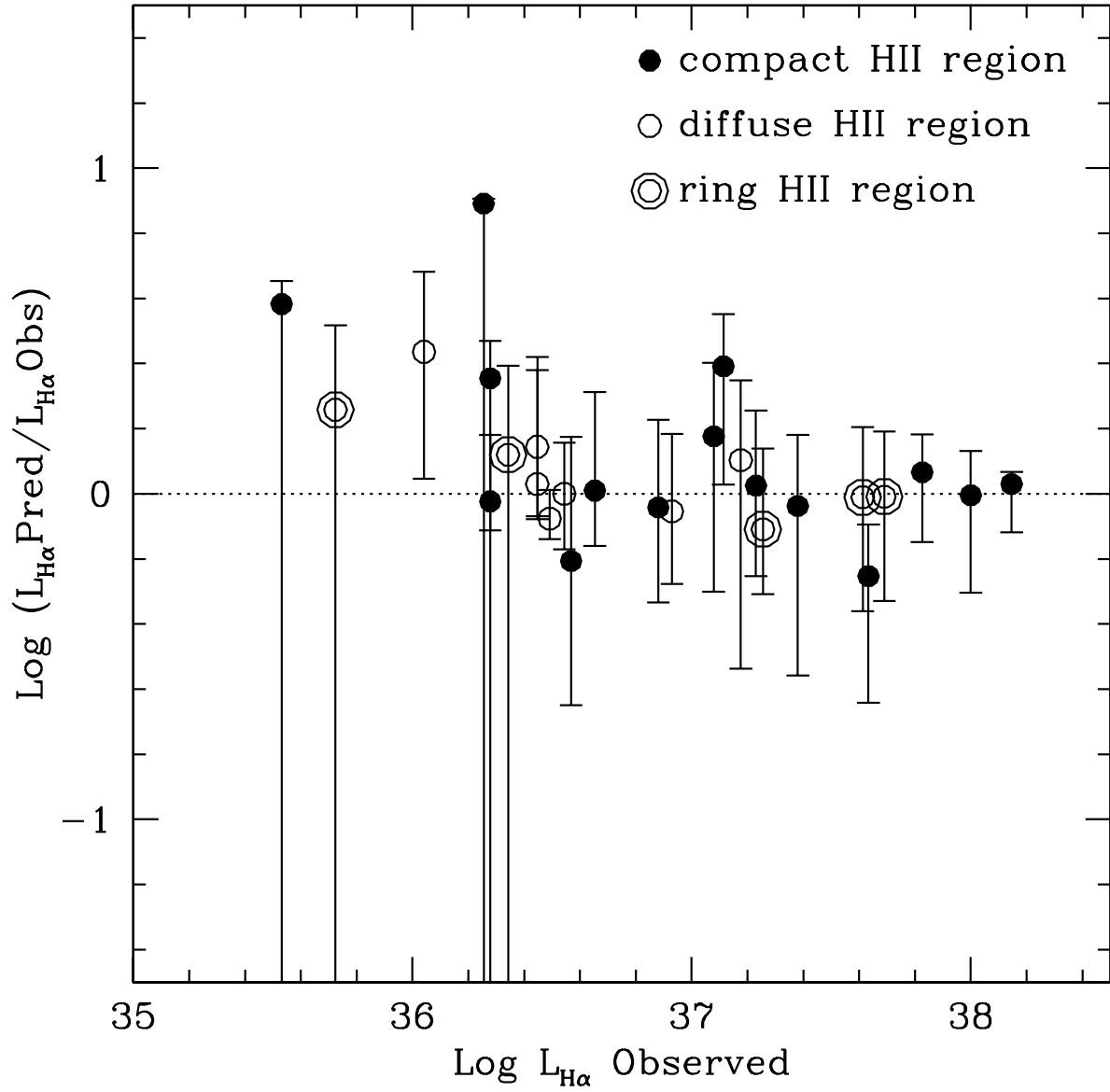


Fig. 6.— Leakiness of HII regions as a function of luminosity. The points are coded by their morphology, with compact HII regions shown as filled circles, diffuse HII regions shown as open circles, and ring-like HII regions shown as double circles.

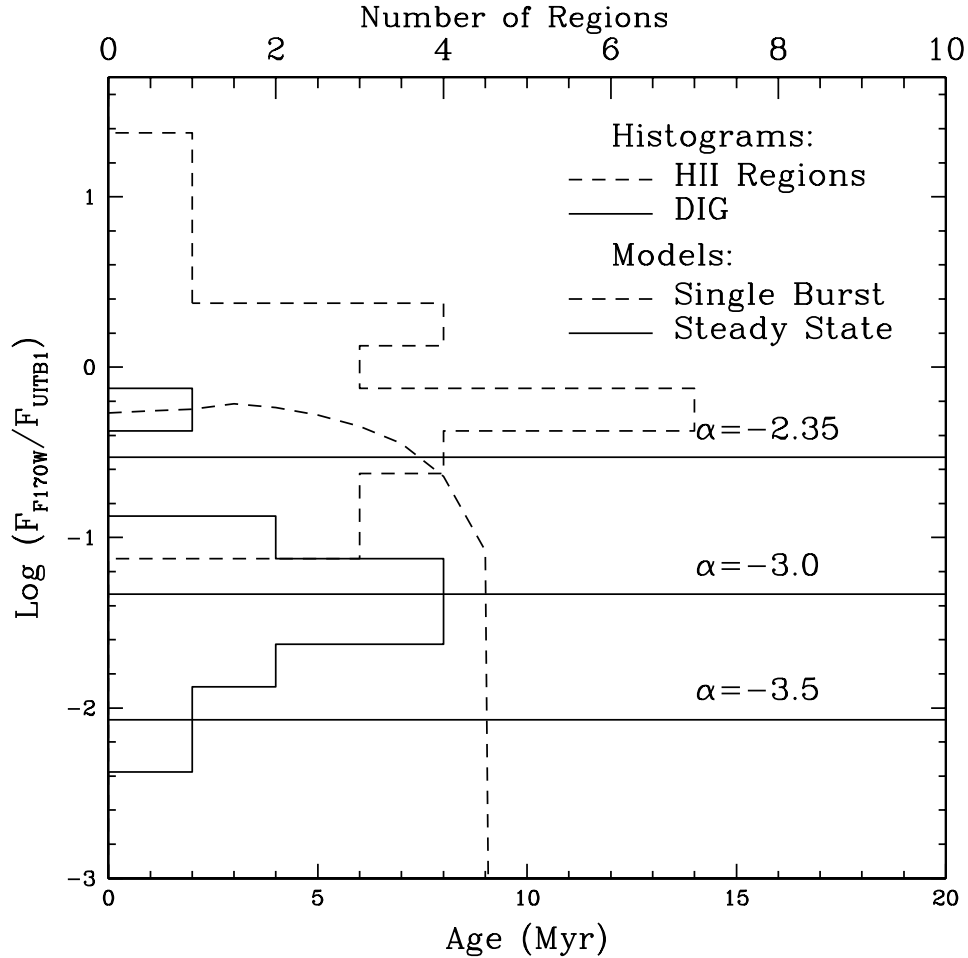


Fig. 7.— Histograms of the FUV flux measured by HST (F_{F170W}) and by UIT (F_{UITB1}), compared to models of the evolution of this ratio with time. The ratio compares the FUV flux from stars of approximately type B0 and earlier (measured in the HST images) to the total FUV flux in the region (measured in the UIT image). HII regions are shown by the dashed histogram, and DIG regions by the solid histogram. The models are from the Starburst99 models (Leitherer *et al.* 1999), and show the behavior of the ratio over time for a single burst model using a Salpeter IMF with slope $\alpha = -2.35$ (dashed line), and the equilibrium ratio for a steady state model with a constant star formation rate (solid line), using IMF slopes $\alpha = -2.35$, -3.0 , and -3.5 for massive stars (these models still use $\alpha = -2.35$ for stars with $M < 20M_{\odot}$). The HST/UIT ratio in the DIG may reflect a steeper IMF for massive stars in the field.

Table 1. Summary of the Data

Band	Central λ (\AA)	FWHM (\AA)	Telescope	Exposure Time (seconds)
H α	6570	30	Burrell Schmidt	20 \times 900
Off-band	6653	68	Burrell Schmidt	20 \times 540
FUV (B1 filter)	1520	354	UIT	424
F170W	1689	434	HST WFPC2	2 \times 900
F336W	2924	727	HST WFPC2	2 \times 900
F439W	4292	464	HST WFPC2	600
F555W	5252	1222	HST WFPC2	160

Table 2. Comparison of Photometric and Spectroscopically Determined Spectral Types^a

Spectral Type	Effective Temperature (K)	$\log g$ (cgs)	Mass (M_{\odot})	Log Q_0 s^{-1}
UIT240 O6-8If ^b				
Best Match ^c	39345	3.62	60.8	49.65
O6Ia	41710	3.69	74.7	49.81
O7Ia	38720	3.58	64.3	49.69
O8Ia	35730	3.46	54.8	49.54
UIT104 Ofpe/WN9 ^b				
Best Match ^c	32257	3.27	49.8	49.31
O8.5Ia	34230	3.40	50.6	49.45
O9Ia	32740	3.33	46.7	49.33
O9.5Ia	31240	3.27	43.1	49.17

^aStellar properties from Vacca, Garmany, & Shull (1996).

^bIdentification and spectral type from Massey *et al.* (1996).

^cBest match to the CoStar models (Schaerer & de Koter 1997).

Table 3. Global Ratios

	$L_{H\alpha}(\text{Obs})^a$ (erg s^{-1})	$L_{H\alpha}(\text{Pred})/L_{H\alpha}(\text{Obs})$	No. of Regions
Four filters required			
All HII Regions	5.85×10^{38}	1.07 ± 0.26	27
HII $L_{H\alpha} \leq 5 \times 10^{36} \text{ erg s}^{-1}$	3.02×10^{37}	1.60 ± 0.60	13
HII $5 \times 10^{36} < L_{H\alpha} \leq 5 \times 10^{37} \text{ erg s}^{-1}$	2.48×10^{38}	1.01 ± 0.41	11
HII $L_{H\alpha} > 5 \times 10^{37} \text{ erg s}^{-1}$	3.07×10^{38}	1.07 ± 0.35	3
All DIG Regions	4.02×10^{38}	0.40 ± 0.12	15
Optical filters only (UBV)			
All HII Regions	5.83×10^{38}	1.80 ± 0.40	26
HII $L_{H\alpha} \leq 5 \times 10^{36} \text{ erg s}^{-1}$	2.84×10^{37}	3.66 ± 2.13	12
HII $5 \times 10^{36} < L_{H\alpha} \leq 5 \times 10^{37} \text{ erg s}^{-1}$	2.48×10^{38}	2.39 ± 0.66	11
HII $L_{H\alpha} > 5 \times 10^{37} \text{ erg s}^{-1}$	3.07×10^{38}	1.15 ± 0.49	3
All DIG Regions	4.02×10^{38}	0.89 ± 0.22	15

^aCorrected for extinction.